Strongly Inhibited Rayleigh-Taylor Growth with 0.25-μm Lasers

Mark H. Emery and John H. Gardner
Laboratory for Computational Physics, U.S. Naval Research Laboratory, Washington, D.C. 20375
and
Stephen E. Bodner
Laser Plasma Branch, U.S. Naval Research Laboratory, Washington, D.C. 20375
(Received 30 January 1986)

It is shown through numerical simulation that the Rayleigh-Taylor growth rate for targets accelerated by laser ablation, is reduced below the classical value, $(kg)^{1/2}$, by factors of 3–4 with 0.25-μm laser light. The simulation results are supported by an analytical expression for the growth rates. These results provide further evidence for the viability of high–aspect-ratio shells in direct-drive laser fusion.

PACS numbers: 52.35.Py, 47.20.−k, 52.50.Jm, 52.65.+z

One of the most critical issues facing direct-drive laser fusion is that of hydrodynamic stability. In laser fusion a pellet is imploded by ablation of material from the outer surface. The acceleration of a cold, dense shell by a hot, light blowoff plasma is an unstable arrangement. The Rayleigh-Taylor (RT),[1] or interchange, instability transposes the position of the more dense fluid with the fluid of lower density. This instability is a potential obstacle to laser fusion since it can cause shell fracture, fuel mix, or, in its mildest form, a nonuniform implosion that will reduce the convergence and severely diminish the energy gain of the fusion pellet.

Perhaps the most serious implication of the RT instability is that it ultimately dictates the allowed aspect ratio $R/\Delta R$ (ratio of the distance pushed to the shell thickness). The allowed aspect ratio both fixes the pressure required to drive the shell inward and indirectly determines the efficiency of the energy coupling between the laser and the shell.[2] If the RT instability grows at its classically predicted rate, thick, low–aspect-ratio shells must be used. This, in turn, implies laser intensities at or above the threshold for plasma instabilities and unacceptably low rocket efficiencies. The use of high–aspect ratio shells has been discussed in the literature[3] and thin-walled glass shells have been imploded with a reasonable degree of success.[4]

The allowed aspect ratio for the laser-ablative case is a function of the RT growth rate and the wavelength of the most dangerous mode. Classical theory[1] predicts that an initial perturbation, η_0, on the interface of an unstably stratified fluid in planar geometry will grow as $\eta(t)=\eta_0 e^{\gamma t}$, where $\gamma=(Akg)^{1/2}$, $k=2\pi/\lambda$. Here λ is the wavelength of the perturbation, g is the acceleration, $A=(\rho_h-\rho_l)/(\rho_h+\rho_l)$ is the Atwood number, and ρ_h (ρ_l) is the density of the heavy (light) fluid. ($A\sim 1$ in the laser-ablative case.) If the perturbation wavelength is much smaller than the radius (R_0) of a spherical pellet, then the planar growth rate can be applied, at a first approximation, to spherical geometry. Let us assume that the growth rate for the laser-ablative case is $\epsilon(kg)^{1/2}$, where $\epsilon<1$. If the shell is imploded halfway inward at constant acceleration then the number of e foldings of unstable growth is $\gamma t=\epsilon(2\pi R_0/\lambda)^{1/2}$. Classical, incompressible theory suggests that the most dangerous mode is $\lambda=\Delta R$, the thickness of the shell; for this mode the inner and outer surfaces are strongly coupled. However, numerical simulations have shown that when compressibility and nonlinear effects are taken into account, it is those perturbation wavelengths several times the shell thickness that are most damaging to the implosion process.[5] We set $\lambda=\pi\Delta R$, and the limiting aspect ratio is given by $R_0/\Delta R=\frac{1}{2}(\gamma t/\epsilon)^2$.

This limit is quite severe since an initial aspect ratio of 10 or so can become an in-flight aspect ratio (IFAR) of ~ 150 as a result of compression. Consider a pellet polished so that after compression the largest surface perturbation has an amplitude of ~ 100 Å, and assume that the implosion process can survive six e foldings of RT growth. If the RT instability grows at its classical rate ($\epsilon=1$), then the maximum IFAR is limited to a value less than 20. The initial aspect ratio for this pellet would be about 1.5. The laser intensity required to generate sufficient pressure to accelerate this shell to implosion velocities would be well above the threshold for plasma instabilities. These thick low–aspect-ratio shells would also severely limit the efficiency and gain of a fusion pellet.[6]

Both numerical simulations[7] and experiments[8] with 1-μm laser light indicate that the RT growth rate in the laser-ablative case is about $\frac{1}{2}$ of the classically predicted value ($\epsilon=\frac{1}{2}$). This would allow an IFAR ~ 70, which is marginal at best. Unless the RT growth rate is reduced even further than that obtained with 1-μm laser light, thin, high–aspect-ratio shells will rupture well before the fuel compression stage. It is this enhanced reduction in the growth rate at shorter laser

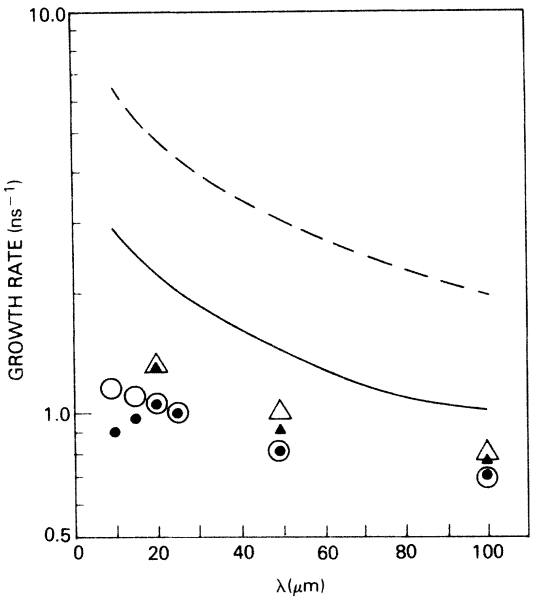

FIG. 1. Comparison of the classical growth rate $[(kg)^{1/2}]$ to the simulation results and to the theoretical results. For the 1-μm case, the solid line is the classical growth rate, solid circles are the simulation results and open circles are the theoretical predictions. For the $\frac{1}{4}$-μm case, the dashed line is the classical growth rate, solid triangles are the simulation results, and open triangles are the theoretical predictions.

wavelengths we wish to discuss in this Letter.

The RT instability is modeled by use of the FAST2D laser-shell simulation code. This is a fully two-dimensional Cartesian code with a sliding Eulerian grid with variable grid spacing. The grid spacing is 0.25 μm for fifteen zones on either side of the ablation layer and increases uniformly to 2 μm for most of the rest of the grid. FAST2D solves the ideal hydrodynamic equations using the flux-corrected-transport algorithms with two-dimensional classical ($T^{5/2}$) plasma thermal conduction. The code has been extensively documented against experimental data[8,9] and is discussed in some detail in Ref. 9 and references cited therein. The initial steady-state density profile is perturbed at its peak with a single sinusoidal mode corresponding to a total initial mass perturbation of less than 0.5%. The laser pulse has a 2-ns Gaussian rise after which the laser intensity is held constant. The computational growth rates are obtained by Fourier transformation of the summed mass of the foil, which is integrated from the rear of the foil to the ablation edge for each transverse coordinate. The growth rate is measured during the constant phase of the laser pulse. Typically six to seven foldings of exponential growth are obtained.

Figure 1 compares the growth rate obtained from the FAST2D simulation to $(kg)^{1/2}$ for 1-μm laser light with an absorbed intensity of 10^{13} W/cm^2 impinging a

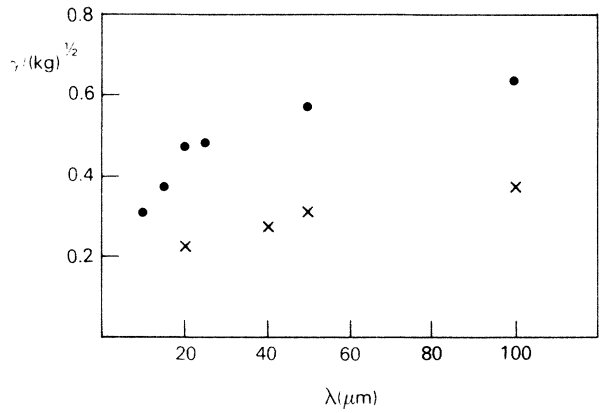

FIG. 2. Ratio of the numerical growth rate to $(kg)^{1/2}$ for 1- (solid circles) and $\frac{1}{4}$-μm (crosses) laser light. The ratio for the 40-μm perturbation wavelength is for an absorbed intensity of 10^{14} W/cm^2.

20-μm-thick plastic (CH) target. The computational growth rates have a $k^{1/2}$ dependence with a moderately strong cutoff for the short-wavelength modes. The computational growth rates are about a factor of 1.5–2 less than the classically predicted value.

The inhibited nature of the RT growth rate for the laser-ablative case is even more apparent for shorter-wavelength lasers. For this case, the laser intensity was increased to a value closer to fusion conditions. Figure 1 also compares the FAST2D simulation results to $(kg)^{1/2}$ for $\frac{1}{4}$-μm laser light with an absorbed laser intensity of 3×10^{14} W/cm^2. The target is a 20-μm-thick plastic (CH) foil. The numerical growth rates for this case are a factor of 3–4 less than the classically predicted values. The ratio of the numerical growth rate to $(kg)^{1/2}$ for both the 1-μm case and the $\frac{1}{4}$-μm case is plotted as a function of perturbation wavelength in Fig. 2. Note that for wavelength perturbations of ~ 60 μm, 3 times the foil thickness, the growth rate has been reduced by a factor of 1.8 for 1-μm lasers and by a factor of 3.5 for $\frac{1}{4}$-μm lasers. Figure 3 compares the density and pressure profiles for both the 1- and $\frac{1}{4}$-μm cases at $t = 3$ ns. The density-gradient scale lengths are 0.49 and 0.40 μm, respectively, and are too small to reduce the RT growth rate by density-gradient stabilization.[10]

The strong dependence of growth rate upon the laser wavelength can be understood in terms of the mechanism that we believe is responsible for the reduction below the classical value: the ablative convection of the vorticity away from the unstable ablation surface.[11] It is the vorticity generated at the unstable interface that controls the interchange of the two fluids. As a result of the laser-ablative process, part of that vorticity is convected away, thereby reducing the growth rate of the instability. If the ablation velocity (V_a) is included in the two-dimensional vorti-

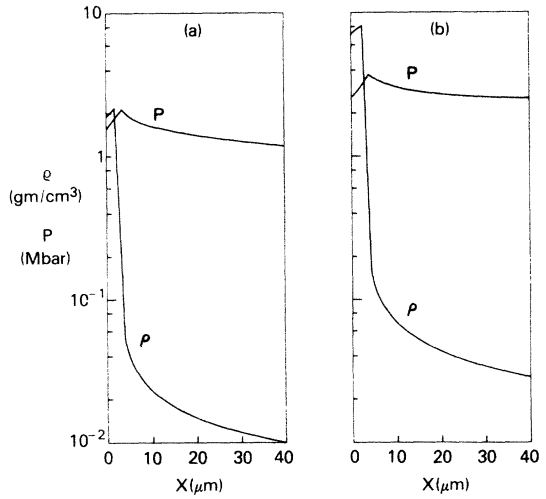

FIG. 3. One-dimensional density and pressure profiles for the cases (a) 1 μm, 10^{13} W/cm^2 and (b) $\frac{1}{4}$ μm, 3×10^{14} W/cm^2 at $t=3$ ns, with a perturbation wavelength of 20 μm. The pressure in (b) is in units of 10 Mbar.

city equation through the convective term, the growth rate for the RT instability in a laser ablatively accelerated target is given by[12]

$$\gamma=[(kV_a/2)^2+\gamma_0^2]^{1/2}-kV_a/2, \quad (1)$$

where $\gamma_0=(kg)^{1/2}$, the classical growth rate. When the ablation velocity is large, the classical RT growth rate is strongly reduced. The above expression is compared to the FAST2D simulation results in Fig. 1. The agreement is quite good for both the 1- and $\frac{1}{4}$-μm cases. The ablation velocities are taken from the numerical simulations and are measured at the center of the unstable shear layer on the ablation front. See Fig. 4. The ablation velocities have the values of 1.3×10^6 cm/s for the 1-μm case, at 10^{13} W/cm^2, and 5.5×10^6 cm/s for the $\frac{1}{4}$-μm case, at 3×10^{14} W/cm^2. The lack of agreement at the short-wavelength perturbations for the 1-μm case is due to the assumption of an infinitely thin vortex sheet at the ablation layer. If γ_0 in Eq. (1) is replaced by the growth rate for an exponential density layer of finite thickness, the cutoff is reproduced.[12]

The strongly inhibited growth for $\frac{1}{4}$-μm lasers is due to a very large ablation velocity. This high mass ablation rate for short-wavelength lasers produces a higher acceleration of plasma away from the target surface, and therefore a larger value of V_a. Figure 5 is a plot of the ablation velocity (V_a) obtained from the FAST2D model as a function of the distance from the target surface for three laser wavelengths (1, $\frac{1}{2}$, and $\frac{1}{4}$ μm). All the calculations were with a 20-μm-thick CH foil with approximately the same isentrope at an absorbed laser intensity of 5×10^{13} W/cm^2. Note that at a distance of $\frac{3}{4}$ μm from the target surface, which is at the center of the unstable shear layer, the ablation

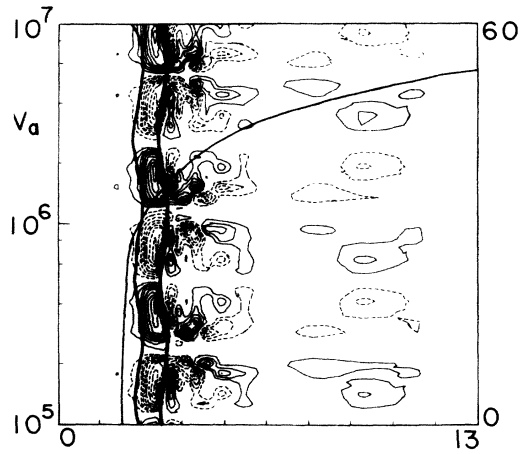

FIG. 4. Isovorticity contours, in 10% increments of the maximum, on the target surface early in the evolution of the 20-μm RT instability for the 1-μm, 10^{13}-W/cm^2 laser case. The laser is impinging on the target from the right. The spatial dimensions are in micrometers. The dashed (solid) contours indicate clockwise (counterclockwise) flow. The wavy bold lines delineate the 10% (right) and 80% (left) density contours. The ablation velocity (V_a, cm/s), which is convecting vorticity away from the target surface, is plotted on top of the vorticity contours. The value of V_a at the center of the layer is 1.3×10^6 cm/s.

velocity for $\frac{1}{4}$-μm light is over 3 times larger than for 1-μm light.

This result can be seen more clearly from a scaling argument. The expansion velocity measured near crit-

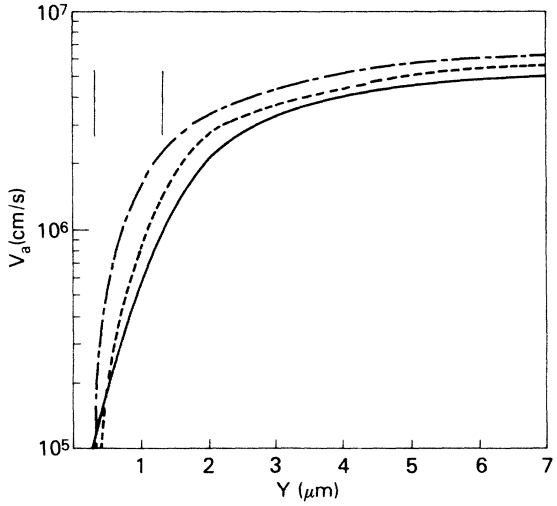

FIG. 5. Ablation velocity (V_a) as a function of distance from the target surface (Y) for 1- (solid), $\frac{1}{2}$- (dashed), and $\frac{1}{4}$-μm (dash-dotted) laser light at 5×10^{13} W/cm^2 impinging on a flat 20-μm-thick plastic (CH) foil. At distances ~40 μm from the target surface, the blowoff velocity of the 1-μm light exceeds that of $\frac{1}{2}$- and $\frac{1}{4}$-μm light. The vertical lines bracket the vortex layer (see Ref. 11).

ical scales as $V_c \propto (I\lambda_l^2)^{1/3}$ and the ablation pressure scales as $P_a \propto (I/\lambda_l)^{2/3}$ in planar geometry,[13] where I is the laser intensity and λ_l is the laser wavelength. From the conservation of mass $\rho_a V_a = \rho_c V_c$, where ρ_a (V_a) is the density (velocity) to be determined very near the ablation layer. Assume that the target and laser profiles can be designed so that the targets are on the same isentrope; i.e., $P_a/\rho_a^{5/3} = \text{const}$, irrespective of laser intensity and wavelength. If the ablation pressure is kept constant as the laser wavelength is reduced, $I \propto \lambda_l$ and the ablation velocity scales as $V_a \propto \lambda_l^{-1}$. If the ablation pressure is allowed to vary then $V_a \propto \lambda_l^{-14/15}$. Thus, although the blowoff velocity at critical decreases with decreasing laser wavelength, the ablation velocity measured near the target surface increases with decreasing laser wavelength. Note that the target acceleration ($g = P_a/M$, where M is the target mass) is constant if the ablation pressure is held fixed and scales as $g \propto \lambda_l^{-2/3}$ if P_a is allowed to vary with laser wavelength. The scaling for the ablation velocity is a stronger function of laser wavelength. The growth rate for the RT instability will then be more strongly inhibited with short-wavelength lasers than with 1-μm laser light, since the vorticity will be convected away at a faster rate.

We have shown that the RT growth rate for laser ablatively accelerated targets is strongly reduced below the classically predicted value for short-wavelength lasers. By combining the most damaging perturbation wavelength of ~ 60 μm, about 3 times the shell thickness, with a growth rate that is 3.5 times smaller than the classical value, $\epsilon \approx 1/3.5$, and up to six e foldings of exponential growth, we conclude that the maximum IFAR for a reactor-sized pellet driven with $\frac{1}{4}$-μm laser light is $R/\Delta R \approx 220$. If one designs for a direct-illumination pellet with an IFAR of order 150 using $\frac{1}{4}$-μm light, then the net (rocket times absorption) efficiency can be as high as 10%.[6] Pellet gains can then be on the order of 200–300, or even higher, depending on other physics constraints.[2] This suggests that high-aspect-ratio shells are indeed a viable and highly attractive design for direct-drive laser fusion. Clearly, we now need additional experimental data on the RT instability under various conditions to test these predictions.

We thank P. C. Reed for her technical assistance. This work was supported by the U.S. Department of Energy and the Office of Naval Research.

[1]Lord Rayleigh, *Theory of Sound* (Dover, New York, 1945), 2nd ed., Vol. 2; G. I. Taylor, Proc. Roy. Soc. London, Ser. A **201**, 192 (1950).

[2]S. E. Bodner, J. Fusion Energy **1**, 221 (1981).

[3]Yu. V. Afanas'ev *et al.*, Pis'ma Zh. Eksp. Teor. Fiz. **21**, 150 (1975) [JETP Lett. **21**, 68 (1975)]; J. D. Lindl and W. C. Mead, Phys. Rev. Lett. **34**, 1273 (1975); M. D. Rosen and J. D. Lindl, Lawrence Livermore National Laboratory Report No. UCRL-50021-83, 1984 (unpublished).

[4]N. G. Basov *et al.*, Pis'ma Eksp. Teor. Fiz. **37**, 109 (1983) [JETP Lett. **37**, 134 (1983)].

[5]M. H. Emery *et al.*, Appl. Phys. Lett. **41**, 808 (1982), and Appl. Phys. Lett. **48**, 1406(E) (1986).

[6]J. H. Gardner and S. E. Bodner, Bull. Am. Phys. Soc. **29**, 1290 (1984); S. E. Bodner *et al.*, Plasma Phys. Controlled Nucl. Fusion Res. **3**, 155 (1984).

[7]C. P. Verdon *et al.*, Phys. Fluids **25**, 1653 (1982); M. H. Emery *et al.*, Phys. Rev. Lett. **48**, 677 (1982), and **56**, 1757(E) (1986).

[8]R. R. Whitlock *et al.*, Phys. Rev. Lett. **52**, 819 (1984); J. Grun *et al.*, Phys. Rev. Lett. **53**, 132 (1984).

[9]M. H. Emery *et al.*, Phys. Rev. Lett. **48**, 253 (1982); P. G. Burkhalter *et al.*, Phys. Fluids **26**, 3650 (1983); M. J. Herbst *et al.*, Phys. Rev. Lett. **52**, 192 (1984).

[10]K. O. Mikaelian and J. D. Lindl, Phys. Rev. A **29**, 290 (1984).

[11]M. H. Emery *et al.*, Phys. Fluids **27**, 1338 (1984).

[12]M. H. Emery, Bull. Am. Phys. Soc. **29**, 1231 (1984), and to be published.

[13]W. M. Manheimer *et al.*, Phys. Fluids **25**, 1644 (1982).